https://ntrs.nasa.gov/search.jsp?R=19710024824 2018-07-23T23:40:35+00:00Z

U. of Iowa 71:23

Distribution of this document is unlimited.

N71-34300
NASA CR 121675

CORRELATED SATELLITE MEASUREMENTS OF LOW-ENERGY ELECTRON PRECIPITATION

AND

GROUND-BASED OBSERVATIONS OF A VISIBLE AURORAL ARC*

by

K. L. Ackerson and L. A. Frank

CASE FILE COPY

Department of Physics and Astronomy
THE UNIVERSITY OF IOWA
Iowa City, Iowa

U. of Iowa 71-23

CORRELATED SATELLITE MEASUREMENTS OF LOW-ENERGY ELECTRON PRECIPITATION

AND

GROUND-BASED OBSERVATIONS OF A VISIBLE AURORAL ARC*

by

K. L. Ackerson and L. A. Frank

July 1971

Department of Physics and Astronomy
The University of Iowa
Iowa City, Iowa 52240

REPRODUCTION IN WHOLE OR IN PART IS PERMITTED
FOR ANY PURPOSE OF THE UNITED STATES GOVERNMENT

*Research supported in part by the National Aeronautics and Space Administration under contracts NAS5-10625, NAS1-8141 and NAS1-2973 and grant NGL16-001-002 and by the Office of Naval Research under contract N000-14-68-A-0196-003.

Distribution of this document is unlimited.

Security Classification

DOCUMENT CONTROL DATA - R&D

(Security classification of title, body of abstract and indexing annotation must be entered when the overall report is classified)

1. ORIGINATING ACTIVITY *(Corporate author)* University of Iowa Department of Physics and Astronomy	2a. REPORT SECURITY CLASSIFICATION UNCLASSIFIED 2b. GROUP

3. REPORT TITLE

Correlated Satellite Measurements of Low-Energy Electron Precipitation and Ground-Based Observations of a Visible Auroral Arc

4. DESCRIPTIVE NOTES *(Type of report and inclusive dates)*

5. AUTHOR(S) *(Last name, first name, initial)*

K. L. Ackerson and L. A. Frank

6. REPORT DATE July, 1971	7a. TOTAL NO. OF PAGES 28	7b. NO. OF REFS 15

8a. CONTRACT OR GRANT NO. N000-14-68-A-0196-003 b. PROJECT NO. c. d.	9a. ORIGINATOR'S REPORT NUMBER(S) U. of Iowa 71-23 9b. OTHER REPORT NO(S) *(Any other numbers that may be assigned this report)*

10. AVAILABILITY/LIMITATION NOTICES

Distribution of this document is unlimited.

11. SUPPLEMENTARY NOTES	12. SPONSORING MILITARY ACTIVITY Office of Naval Research

13. ABSTRACT

SEE PAGES FOLLOWING.

DD FORM 1 JAN 64 1473

Security Classification

Security Classification

14. KEY WORDS	LINK A ROLE	LINK A WT	LINK B ROLE	LINK B WT	LINK C ROLE	LINK C WT
Aurora						
Magnetosphere						
Plasma Sheet						
Radiation Zones						

INSTRUCTIONS

1. ORIGINATING ACTIVITY: Enter the name and address of the contractor, subcontractor, grantee, Department of Defense activity or other organization *(corporate author)* issuing the report.

2a. REPORT SECURITY CLASSIFICATION: Enter the overall security classification of the report. Indicate whether "Restricted Data" is included. Marking is to be in accordance with appropriate security regulations.

2b. GROUP: Automatic downgrading is specified in DoD Directive 5200.10 and Armed Forces Industrial Manual. Enter the group number. Also, when applicable, show that optional markings have been used for Group 3 and Group 4 as authorized.

3. REPORT TITLE: Enter the complete report title in all capital letters. Titles in all cases should be unclassified. If a meaningful title cannot be selected without classification, show title classification in all capitals in parenthesis immediately following the title.

4. DESCRIPTIVE NOTES: If appropriate, enter the type of report, e.g., interim, progress, summary, annual, or final. Give the inclusive dates when a specific reporting period is covered.

5. AUTHOR(S): Enter the name(s) of author(s) as shown on or in the report. Enter last name, first name, middle initial. If military, show rank and branch of service. The name of the principal author is an absolute minimum requirement.

6. REPORT DATE: Enter the date of the report as day, month, year; or month, year. If more than one date appears on the report, use date of publication.

7a. TOTAL NUMBER OF PAGES: The total page count should follow normal pagination procedures, i.e., enter the number of pages containing information.

7b. NUMBER OF REFERENCES: Enter the total number of references cited in the report.

8a. CONTRACT OR GRANT NUMBER: If appropriate, enter the applicable number of the contract or grant under which the report was written.

8b, 8c, & 8d. PROJECT NUMBER: Enter the appropriate military department identification, such as project number, subproject number, system numbers, task number, etc.

9a. ORIGINATOR'S REPORT NUMBER(S): Enter the official report number by which the document will be identified and controlled by the originating activity. This number must be unique to this report.

9b. OTHER REPORT NUMBER(S): If the report has been assigned any other report numbers *(either by the originator or by the sponsor)*, also enter this number(s).

10. AVAILABILITY/LIMITATION NOTICES: Enter any limitations on further dissemination of the report, other than those imposed by security classification, using standard statements such as:

(1) "Qualified requesters may obtain copies of this report from DDC."

(2) "Foreign announcement and dissemination of this report by DDC is not authorized."

(3) "U. S. Government agencies may obtain copies of this report directly from DDC. Other qualified DDC users shall request through _____."

(4) "U. S. military agencies may obtain copies of this report directly from DDC. Other qualified users shall request through _____."

(5) "All distribution of this report is controlled. Qualified DDC users shall request through _____."

If the report has been furnished to the Office of Technical Services, Department of Commerce, for sale to the public, indicate this fact and enter the price, if known.

11. SUPPLEMENTARY NOTES: Use for additional explanatory notes.

12. SPONSORING MILITARY ACTIVITY: Enter the name of the departmental project office or laboratory sponsoring *(paying for)* the research and development. Include address.

13. ABSTRACT: Enter an abstract giving a brief and factual summary of the document indicative of the report, even though it may also appear elsewhere in the body of the technical report. If additional space is required, a continuation sheet shall be attached.

It is highly desirable that the abstract of classified reports be unclassified. Each paragraph of the abstract shall end with an indication of the military security classification of the information in the paragraph, represented as *(TS)*, *(S)*, *(C)*, or *(U)*.

There is no limitation on the length of the abstract. However, the suggested length is from 150 to 225 words.

14. KEY WORDS: Key words are technically meaningful terms or short phrases that characterize a report and may be used as index entries for cataloging the report. Key words must be selected so that no security classification is required. Identifiers, such as equipment model designation, trade name, military project code name, geographic location, may be used as key words but will be followed by an indication of technical context. The assignment of links, roles, and weights is optional.

DD FORM 1 JAN 64 1473 (BACK)

Security Classification

Abstract

A comparison of low-energy charged particle intensities measured with the low-altitude satellite Injun 5 and a ground-based observation of an auroral arc at Fort Churchill on 21 December 1968 during late local evening has established that an intense precipitation band of electron intensities provides the primary energy influx for the auroral light. This precipitation event was located poleward of and adjacent to the trapping boundary for more energetic electron ($E > 45$ keV) intensities. The peak energy fluxes were ~ 10 ergs $(cm^2\text{-sec-sr})^{-1}$ directed along the local magnetic field direction into the earth's atmosphere. Proton and electron intensities similar to those in the plasma sheet in the magnetotail were observed in a substantially less intense zone positioned equatorward of and adjacent to the trapping boundary. Angular distributions of these particle intensities from the plasma sheet were peaked at pitch angles perpendicular to the local magnetic field.

The intense precipitation band of electron intensities poleward of the trapping boundary is interpreted as the signature of direct acceleration of magnetosheath electrons into the earth's atmosphere. The plasma sheet proton and electron intensities observed equatorward of the trapping boundary are identified as the 'debris' from this intense precipitation band located adjacent to the trapping boundary.

I. Introduction

Simultaneous observations of the auroral lights and their association with precipitating electron and proton intensities are essential for eventual delineation of the mechanisms responsible for these phenomena. Low-altitude rockets capable of comprehensive measurements of low-energy charged particle intensities have been launched directly into visible aurora [cf. Evans, 1969]. However, the spatial coverage of these rocket trajectories appears to be inadequate for determination of such features as the 'trapping boundary' for energetic electrons, the proton ring current, the plasma sheet and the high-latitude magnetotail relative to the auroral light emissions. Coordinated observations of auroral emissions with photometers borne on aircraft and of precipitating low-energy charged particles on polar orbiting, low-altitude satellites also have been reported [cf. Meyerott and Evans, 1969], but again these results were insufficient for identifying the topological features of the magnetospheric plasma distributions with the low-altitude phenomena. Vasyliunas [1970] has been able to identify auroral arcs in all-sky camera pictures with the inner edge of the plasma sheet as measured with a low-energy electron detector at higher altitudes with OGO-1.

We report here comprehensive observations of low-energy electron and proton intensities with the polar orbiting, low-altitude satellite Injun 5 over a visual auroral arc as recorded simultaneously by an all-sky camera at Fort Churchill, Manitoba, Canada. The particle observations are sufficient in energy range and temporal resolution for determination of the 'trapping boundary' for energetic electrons and of the low-altitude signatures of the plasma sheet and the proton ring current. One of the most interesting conclusions of this comparison of measurements is that the magnetic field lines threading the visual auroral arc are not topologically extended into the plasma sheet in the distant magnetosphere. This result is in agreement with interpretations of recent observations of plasmas in the earth's distant polar magnetosphere and at low altitudes over the auroral zones [Frank, 1971a, b; Frank and Gurnett, 1971]. For a discussion of simultaneous measurements of very-low-frequency radio noise during the series of particle observations reported here the reader is referred to the companion paper by Mosier and Gurnett [1971].

II. Observations

Our measurements of the low-energy proton and electron intensities over a visual auroral arc were obtained with an array of electrostatic analyzers on the polar orbiting, low-altitude satellite Injun 5. This satellite was magnetically aligned and was injected into an orbit with initial apogee and perigee altitudes 2528 and 677 km, respectively, and inclination 81°. The altitude of the following observations was $\sim$ 2250 km and the corresponding magnetic local time was $\sim$ 1930 (local evening). The instrumentation could be operated in a variety of modes controlled by ground command. For the present series of observations the Low Energy Proton and Electron Differential Energy Analyzers (LEPEDEA's) provided 117-point differential energy spectrums of trapped and precipitated proton and electron intensities, simultaneously and separately, in a 970-millisecond sampling interval once each two seconds. The corresponding proton and electron energy ranges were $40 \leq E \leq 12{,}000$ eV and $50 \leq E \leq 15{,}000$ eV, respectively, for this instrument operating mode. Directional, integral intensities of more energetic electrons, $E > 45$ keV, were measured with an accompanying array of collimated, thin-windowed Geiger-Mueller tubes. Further details concerning the satellite and

instrumentation have been given by Frank and Ackerson [1971].

All-sky camera pictures of the auroral arc taken at Fort Churchill on 21 December 1968 are presented in Figure 1. Due to the low contrast of the original photographs these observations have been reproduced by line drawings [Mosier and Gurnett, 1971]. The magnetic field line passing through the satellite position has been traced down to an altitude of 100 km for each all-sky camera frame. This intersection of the field line with the surface at 100 km altitude is indicated by the dots near the western limb of each line drawing in Figure 1. The satellite clearly passed over a single, well-defined auroral arc. Further discussion of these all-sky camera observations is given by Mosier and Gurnett [1971]. The magnetic index K_p was 0 for the three-hour period (2100 to 2400 U.T.) preceding this pass and 3^- for the period during the observations.

Corresponding observations of the precipitated electron intensities over the energy range 50 to 15,000 eV are displayed in the color-coded, energy-time (E-t) spectrogram in Plate 1a. The ordinate scale is electron energy in units of eV and the abscissa is Universal Time [Frank and Ackerson, 1971]. The detector response is color coded from blue to red (low to high responses) at each point in the E-t plane. A color calibration strip for the $\log_{10}$ of the detector response in counts $(\text{second})^{-1}$ is provided at the

right-hand side of the graph. Magnetic invariant latitude (Λ), magnetic field magnitude (B) at the satellite position and corresponding magnetic local time (MLT) are given at the bottom of Plate 1a.

Examination of the electron precipitation pattern shown in Plate 1a reveals a single intense event over the time period 0152:32 to 0153:00 U.T. and an adjacent equatorward band of substantially lesser intensities at 0153:00 to 0153:45 U.T. The intense event is of the type designated as 'inverted V' precipitation bands as described by Frank and Ackerson [1971]. These precipitation events are usually characterized by electron average energies which increase to a maximum energy and subsequently decrease as the satellite passes through these regions. The angular distributions are often highly anisotropic favoring small pitch angles directed into the atmosphere; and peak directional intensities are typically $\geqslant 10^9$ electrons $(cm^2\text{-sec-sr})^{-1}$ [Frank and Gurnett, 1971; Frank and Ackerson, 1971]. For the low-energy 'inverted V' event of Plate 1a the average electron energy ranged from $\sim$ 100 eV to 670 eV, the peak directional intensities were 4×10^9 $(cm^2\text{-sec-sr})^{-1}$ and the peak number density was 4.5 $(cm^3\text{-sr})^{-1}$.

Several selected differential energy spectrums for this intense precipitation band are shown in Figure 2.

Trapped and precipitated electron intensities, measured simultaneously, are compared. As Universal Time increases, the satellite is moving equatorward and the corresponding angular distributions are highly anisotropic near the poleward edge of the event and progress toward isotropy as the satellite approaches the equatorward boundary.

The intense 'inverted V' precipitation band of Plate 1a coincides with the passage of the satellite over the visual auroral arc shown in Figure 1 within the temporal accuracy of the combined observations. The trapped and precipitated electron energy fluxes displayed in the bottom half of Figure 3 provide a further basis of comparison and summarize the pitch angle anisotropies for this series of measurements. Note that at 0152:41 U.T., the electron energy fluxes parallel to the local magnetic field (precipitated) exceeded those for electrons with perpendicular pitch angles (trapped) by factors ~ 50. During this time period the aurora brightened beneath the satellite (see Figure 1).

The gross character of the relatively weak electron precipitation band adjacent to and equatorward of the main precipitation event will be of interest to us in later discussion (see Plate 1a at $\sim$ 0153:00 to 0153:45 U.T.). The angular distributions are peaked at pitch angles

perpendicular to the magnetic field, trapped energy fluxes are $\sim 7 \times 10^{-2}$ erg $(cm^2\text{-sec-sr})^{-1}$, and corresponding precipitated electron energy fluxes are $\sim 10^{-2}$ erg $(cm^2\text{-sec-sr})^{-1}$. Average electron energies range from $\sim$ 150 to 350 eV and number densities for the trapped electron intensities are $\sim 2 \times 10^{-2}$ $(cm^3\text{-sr})^{-1}$. These energy fluxes, average energies and number densities for the trapped electron intensities in this lesser precipitation zone are not largely dissimilar to those reported for soft electron spectrums in the plasma sheet at 18 R_E (R_E, earth radius) by Hones et al [1971].

The simultaneous observations of electron $E > 45$ keV intensities provide further evidences as to the relationship of these low-energy electron zones to the distant magnetosphere. Trapped and precipitated electron intensities are summarized in the upper half of Figure 3. The 'trapping boundary' for energetic electrons is encountered at 0153:00 (± 10 seconds). This trapping boundary has been previously interpreted by Frank and Gurnett [1971] as delineating the position of the last closed field line, i.e., all field lines above this 'trapping boundary', as viewed with a detector with generous geometric factor, are open to the interplanetary medium. The intense inverted 'V' precipitation band is located poleward and adjacent to the trapping boundary and the less intense zone of lower energy

electrons is positioned equatorward of this boundary (compare Figure 3 with Plate 1a). Measurable intensities of higher energy electrons $E > 45$ keV precipitated into the atmosphere are observed within this less intense zone.

Thus far our presentation strongly favors identifying the lower-intensity electron band encountered over 0153:00 to 0153:45 U.T. in Plate 1a with the plasma sheet in the magnetotail. Simultaneous observations of proton intensities over the energy range $40 \leq E \leq 12{,}000$ eV confirms this identification. An E-t spectrogram for trapped proton intensities is shown in Plate 1b. The proton intensities are low, but the location of measurable intensities is readily discernible. Proton intensities above the instrument mode threshold are encountered over 0153:00 to $\sim$ 0154:10 U.T. The average proton energy increases as the satellite moves equatorward. This proton zone is bounded on the poleward side by the trapping boundary and extends equatorward of the lower intensity electron band which we have identified with plasma sheet electron intensities. The proton intensities at the equatorward boundary, $\sim 10^7$ $(cm^2\text{-sec-sr})^{-1}$, are similar to those for the quiet-time ring current at the magnetic equator [cf. Frank, 1967]. We identify this proton band as the low altitude signature of the plasma sheet and ring current proton intensities. In fact the poleward

termination of plasma sheet electron intensities relative to that of the proton intensities is a direct signature of their spatial relationship as measured at the magnetic equator in this local time sector during relative magnetic quiescence [Frank, 1971c].

III. Discussion

Our comparison of low-energy charged particle intensities measured with the low-altitude satellite Injun 5 and a ground-based observation of an auroral arc has clearly established that an 'inverted V' precipitation band of electron intensities of the type previously described by Frank and Ackerson [1971] provides the primary energy influx for the auroral light. This electron precipitation band at late local evening was $\sim$ 110 km in latitudinal width and was positioned poleward of and adjacent to the 'trapping boundary' for more energetic electron ($E > 45$ keV) intensities.

A considerably less intense band of electron intensities was located equatorward of and adjacent to the energetic electron trapping boundary. The energy fluxes, average energies and intensities of protons and electrons in this region were not largely dissimilar to those observed in the plasma sheet [cf. Eather and Mende, 1971]. No measurable intensities of protons were observed in the intense 'inverted V' precipitation band located poleward of the trapping boundary. Peak energy fluxes above and below the trapping boundary were $\sim$ 10 and 0.1 erg $(cm^2\text{-sec-sr})^{-1}$, respectively. Large field-aligned electron intensities were observed above the trapping boundary whereas electron

intensities were peaked at pitch angles perpendicular to the local magnetic field for lower latitudes. In view of all these evidences we identify the relatively weak proton and electron bands spanning 0153:00 to ~ 0154:10 U.T. of Plates 1a and 1b as the low-altitude signature of the plasma sheet and ring current at the magnetic equator.

Recently we have presented further evidences that the trapping boundary for energetic electrons as observed here with a detector of generous geometric factor is coincident with the boundary between magnetic field lines closed within the magnetosphere and open field lines to the interplanetary medium [Frank, 1971a, b; Frank and Gurnett, 1971]. Hence field lines threading the intense electron precipitation band during 0152:32 to 0153:00 of Plate 1a are connected to interplanetary magnetic field lines. More specifically these field lines are mapped into the downstream magnetosheath adjoining the plasma sheet [Frank, 1971a; Frank and Gurnett 1971]. The number densities, 2 to 4 $(cm^3\text{-}sr)^{-1}$, and directional intensities, $\sim 4 \times 10^9$ $(cm^2\text{-}sec\text{-}sr)^{-1}$, are similar to those typically observed in the magnetosheath. We have previously reported and interpreted simultaneous observations of convection electric fields, 'inverted V' precipitation events, very-low-frequency electromagnetic noise and the energetic trapping boundary in

terms of an auroral acceleration mechanism operative at altitudes $\sim$ 1 to 5 R_E within the 'inverted V' electron precipitation bands [Frank and Ackerson, 1971; Frank and Gurnett, 1971; Gurnett and Frank, 1971]. Hence we again interpret our observations of this intense precipitation band as the signature of direct acceleration of magnetosheath electrons into the earth's atmosphere via a dynamo driven by the flow of magnetosheath plasma past the earth.

The plasma sheet in the earth's magnetotail is characterized by electrons with higher average energy and considerably less density relative to those of the magnetosheath surrounding the plasma sheet. Vasyliunas [1971] has stressed that an understanding of the origins of the plasma sheet rests importantly on a proper interpretation of the differences of the electron populations in these two plasma regions. Returning to Plate 1a we assume that reconnection of magnetic field lines is occurring in the vicinity of the trapping boundary at 0153:00 U.T. [Frank, 1971a] and note that (1) the average electron energies just above and below the trapping boundary are similar, (2) the directional intensities range up to two orders of magnitude higher above the trapping boundary relative to those equatorward of the boundary, (3) the angular distributions are field-aligned poleward of the trapping boundary, approximately isotropic

near the boundary (over the upward hemisphere of pitch angles) and peaked perpendicular to the magnetic field below the trapping boundary, and (4) measurable proton intensities are observed only equatorward of the trapping boundary. Then we can only reasonably conclude that the intense electron precipitation event associated with the visible arc is not the product of an acceleration mechanism within the plasma sheet but that the plasma sheet proton and electron intensities are the debris which has been trapped on newly reconnected field lines from 'inverted V' events located adjacent to the trapping boundary.

It is of interest to note here the results of our recent preliminary inspection of extended series of E-t spectrograms of auroral precipitation patterns in search of events which could be attributed primarily to an influx of plasma sheet electrons. These events do occur and appear to be related to magnetospheric substorms. An example of such an event is given in Plate 4b in the paper by Frank and Ackerson [1971]. The electron precipitation pattern is broad in latitudinal width, relatively structureless, and located equatorward of the trapping boundary.

For some electron precipitation patterns, the 'trapping boundary' for electrons E > 45 keV, which we utilize as a natural coordinate for most of our low-altitude observations at high latitudes, is not readily determined

when the 'inverted V' electron bands rise in average energy to $\geqslant$ 10 keV. This difficulty was not encountered for the E-t spectrogram shown in Plate 1a since the average electron energies are less than 1 keV. For precipitation patterns with clearly definable trapping boundaries the 'inverted V' electron bands, single or multiple, are positioned poleward of the trapping boundary. Often one of these bands is located adjacent to the trapping boundary. However, for the 'inverted V' event shown in Plate 5a of Frank and Ackerson [1971] with peak energy fluxes $\sim$ 80 ergs $(cm^2\text{-sec-sr})^{-1}$ during a magnetic storm, large intensities of electrons $E > 45$ keV, $\geqslant 5 \times 10^6$ $(cm^2\text{-sec-sr})^{-1}$, were produced by the acceleration mechanism. The angular distributions of these more energetic electron intensities approached isotropy. Hence it appears that 'inverted V' electron events can also provide large increases of electron intensities with energies above the thresholds of commonly flown thin-windowed G. M. tubes during periods of relative magnetic disturbance. These acceleration events could provide the rapid and dramatic increases of outer zone electron ($E > 40$ keV) intensities observed during these magnetic conditions [cf. Owens and Frank, 1968].

Acknowledgments

The authors wish to express their appreciation to the superintendent and the Auroral Observatory staff of the Churchill Research Range for providing the all-sky camera pictures used in this correlative study. This research was supported in part by the National Aeronautics and Space Administration under contracts NAS5-10625, NAS1-8141, NAS1-2973 and grant NGL16-001-002 and by the Office of Naval Research under contract N000-14-68-A-0196-003.

References

Eather, R. H. and S. B. Mende, High latitude particle precipitation, and source regions in the magnetosphere; Paper presented at Advanced Study Institute on Magnetosphere - Ionosphere Interactions, Dalseter, Norway, 1971.

Evans, D. S., Fine structure in the energy spectrum of low-energy auroral electrons; Atmospheric Emissions, ed. by B. M. McCormac and A. Omholt, Reinhold Publishing Company, 107-118, 1969.

Frank, L. A., On the extraterrestrial ring current during geomagnetic storms; J. Geophys. Res., 72, 3753-3767, 1967.

Frank, L. A., Comments on a proposed magnetospheric model; J. Geophys. Res., 76, 2512-2515, 1971a.

Frank, L. A., Plasma in the earth's polar magnetosphere; J. Geophys. Res. (accepted for publication), 1971b.

Frank, L. A., Relationship of the plasma sheet, ring current, trapping boundary, and plasmapause near the magnetic equator and local midnight; J. Geophys. Res., 76, 2265-2275, 1971c.

Frank, L. A. and K. L. Ackerson, Observations of charged particle precipitation into the auroral zone; J. Geophys. Res., 76, 3612-3643, 1971.

Frank, L. A. and D. A. Gurnett, On the distributions of plasmas and electric fields over the auroral zones and polar caps; J. Geophys. Res. (accepted for publication), 1971.

Gurnett, D. A. and L. A. Frank, VLF radio noise and plasma observations in the auroral zone; J. Geophys. Res. (submitted for publication), 1971.

Hones, E. W., J. R. Asbridge, S. J. Bame and S. Singer, Energy spectra and angular distributions of particles in the plasma sheet and their comparison with rocket measurements over the auroral zone; J. Geophys. Res., 76, 63-87, 1971.

Meyerott, R. E. and J. E. Evans, Coordinated measurements of particles, luminosity, and electron concentrations; Atmospheric Emissions, ed. by B. M. McCormac and A. Omholt, Reinhold Publishing Company, 119-130, 1969.

Mosier, S. R. and D. A. Gurnett, Observed correlations between auroral and VLF emissions; J. Geophys. Res. (submitted for publication), 1971.

Owens, H. D. and L. A. Frank, Electron omnidirectional intensity contours in the earth's outer radiation zone at the magnetic equator; J. Geophys. Res. 73, 199-208, 1968.

Vasyliunas, V. M., Relation of the plasma sheet to the auroral oval; (abstract), EOS, 51, 814, 1970.

Vasyliunas, V. M., Thermal and suprathermal plasmas in the magnetosphere; Comments Astrophys. Space Phys., 3 (2), 48-52, 1971.

Figure Captions

Plate 1a. A color-coded energy-time (E-t) spectrogram for precipitated electron intensities over Fort Churchill, Canada, on 21 December 1968. The abscissa and ordinate are Universal Time and electron energy, respectively. The detector responses are coded via a curve in the color solid, i.e., blue (low electron intensities) through red (high electron intensities).

Plate 1b. Continuation of Plate 1a for simultaneous measurements of low-energy trapped proton intensities.

Figure 1. Line reproductions of all-sky camera photographs at Fort Churchill, Manitoba, Canada on 21 December 1968. The solid circles accompanied by arrows indicate the intersections of the magnetic field lines passing through the instantaneous satellite positions with a surface at an altitude of 100 kilometers (after Mosier and Gurnett [1971]).

Figure 2. Several directional, differential energy spectrums for trapped and precipitated electron intensities observed on 21 December 1968 (see Plate 1a).

Figure 3. Directional intensities of electrons $E > 45$ keV (top panel) and of directional energy fluxes of lower energy electrons $50 \leq E \leq 15{,}000$ eV (bottom panel) for a segment of the time period covered by Plates 1a and 1b.

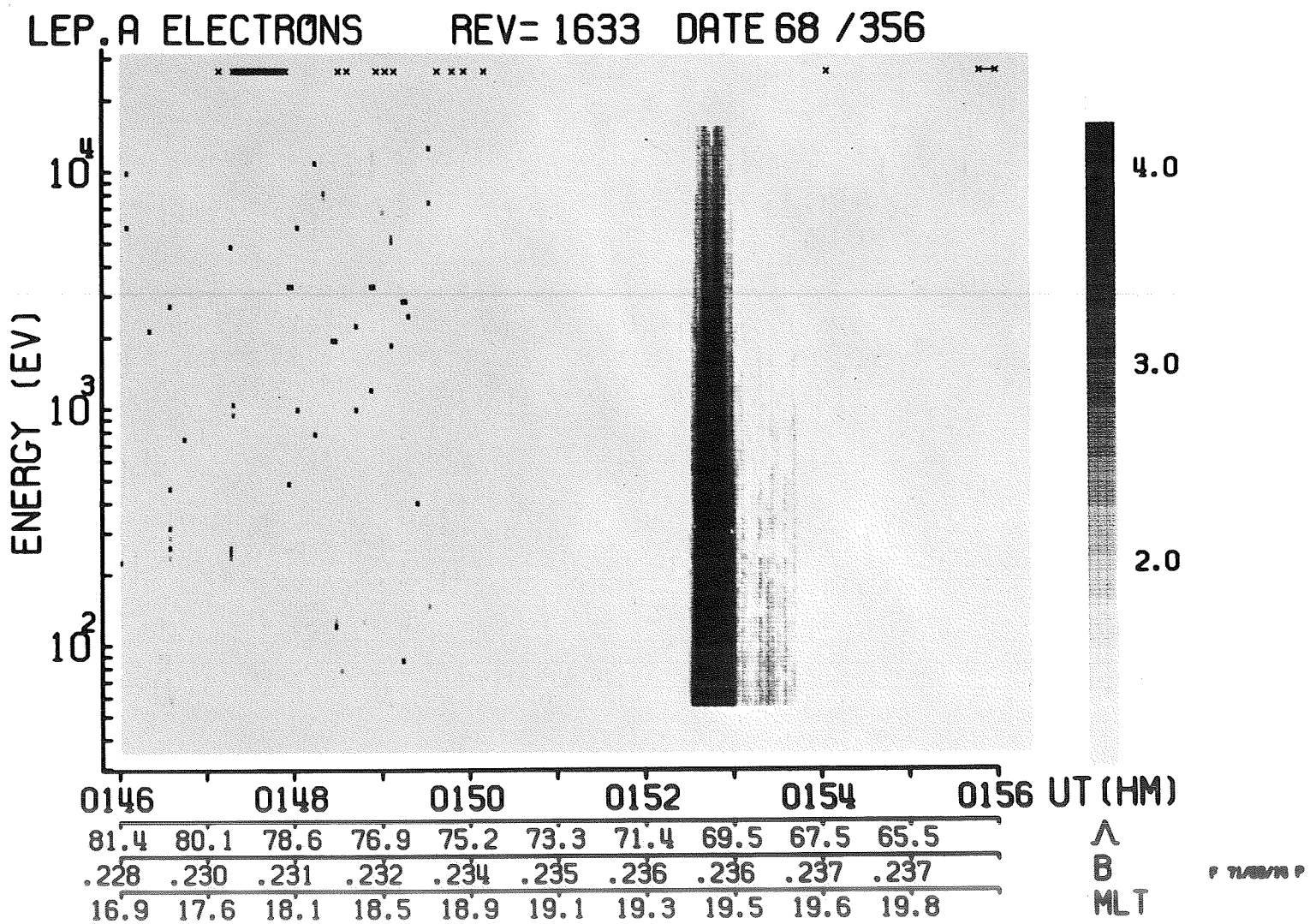
LEP.A ELECTRONS REV= 1633 DATE 68 /356
ENERGY (EV)
10^4
10^3
10^2
4.0
3.0
2.0
0146 0148 0150 0152 0154 0156 UT (HM)
81.4 80.1 78.6 76.9 75.2 73.3 71.4 69.5 67.5 65.5
Λ
.228 .230 .231 .232 .234 .235 .236 .236 .237 .237
B
16.9 17.6 18.1 18.5 18.9 19.1 19.3 19.5 19.6 19.8
MLT

Plate 1a.

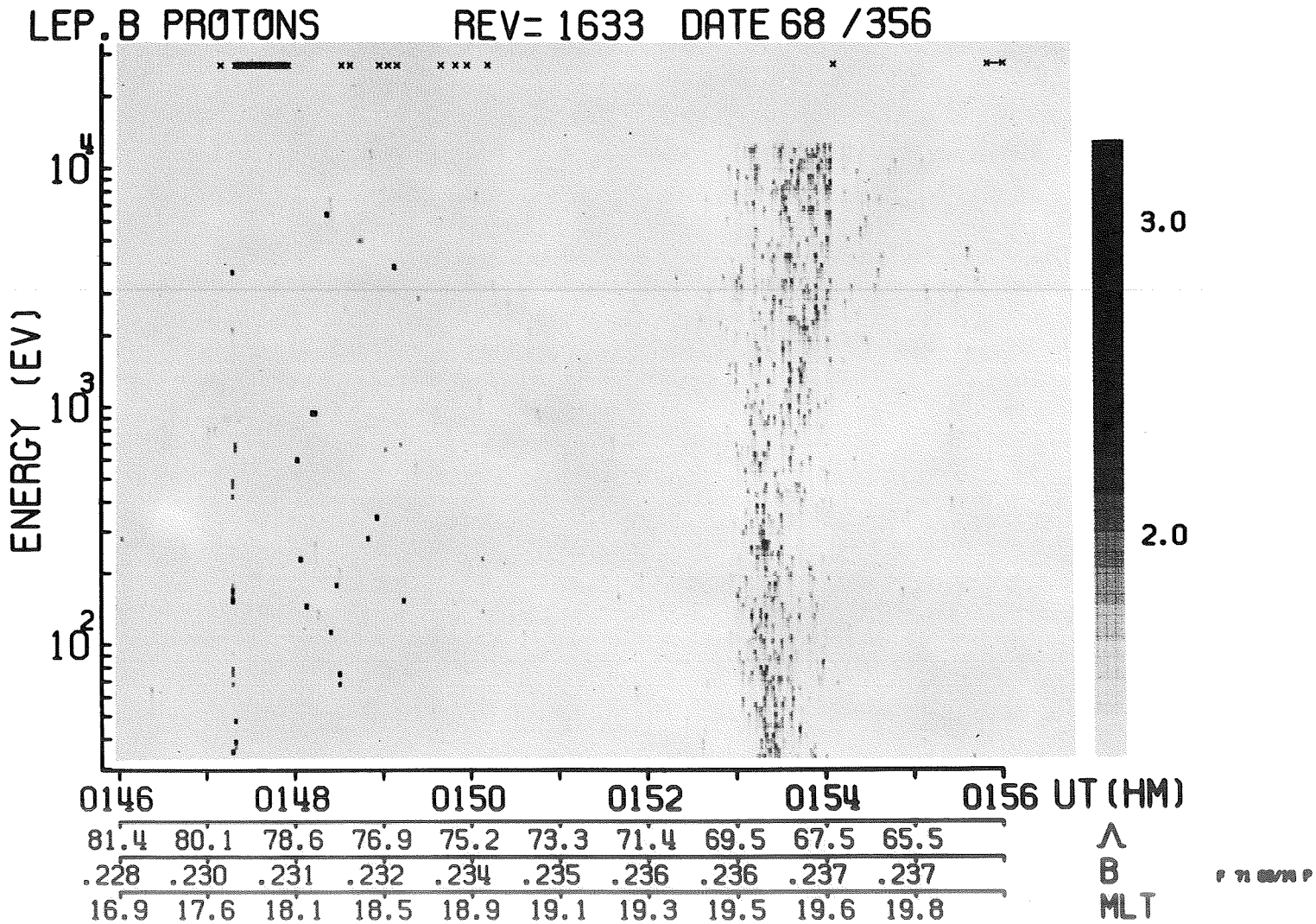
LEP.B PROTONS REV= 1633 DATE 68 /356
ENERGY (EV)
10^4
10^3
10^2
3.0
2.0
0146 0148 0150 0152 0154 0156 UT (HM)
81.4 80.1 78.6 76.9 75.2 73.3 71.4 69.5 67.5 65.5 Λ
.228 .230 .231 .232 .234 .235 .236 .236 .237 .237 B
16.9 17.6 18.1 18.5 18.9 19.1 19.3 19.5 19.6 19.8 MLT

Plate 1b.

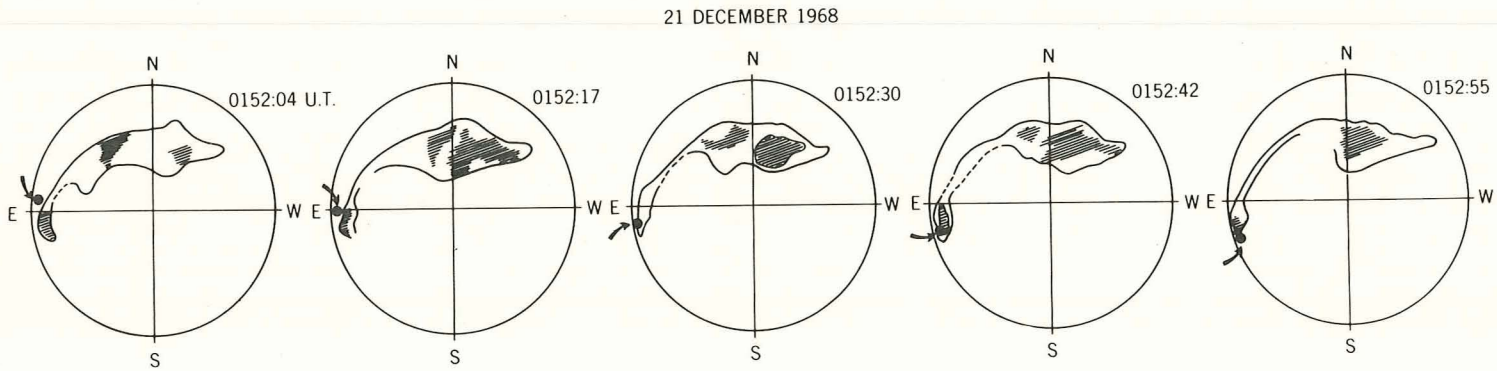
21 DECEMBER 1968
N
S
E
W
0152:04 U.T.
0152:17
0152:30
0152:42
0152:55

Figure 1.

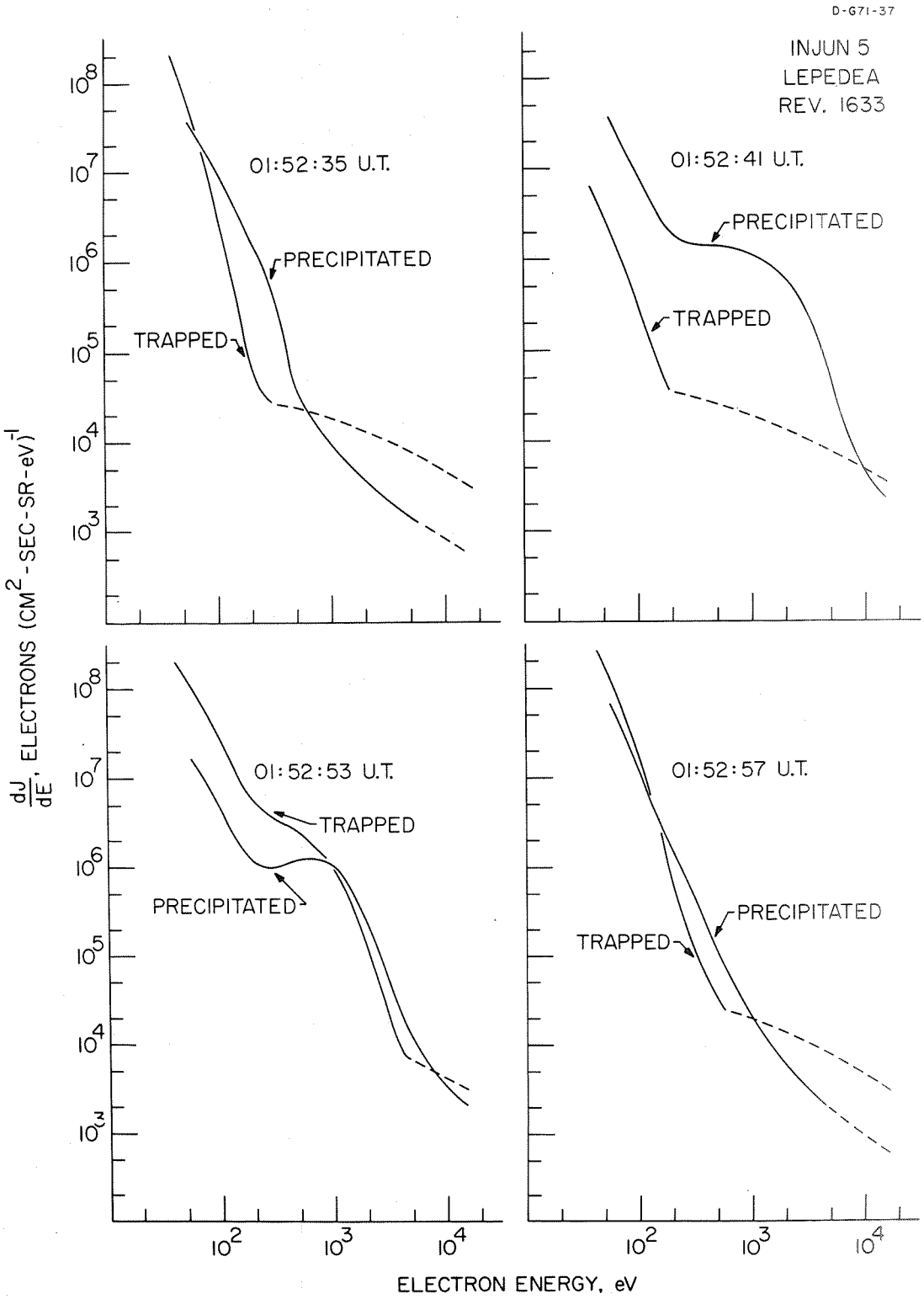
D-G71-37
INJUN 5
LEPEDEA
REV. 1633
01:52:35 U.T.
PRECIPITATED
TRAPPED
01:52:41 U.T.
PRECIPITATED
TRAPPED
01:52:53 U.T.
TRAPPED
PRECIPITATED
01:52:57 U.T.
PRECIPITATED
TRAPPED
$\frac{dJ}{dE}$, ELECTRONS (CM^2-SEC-SR-eV)$^{-1}$
10^8
10^7
10^6
10^5
10^4
10^3
10^2
10^3
10^4
ELECTRON ENERGY, eV

Figure 2.

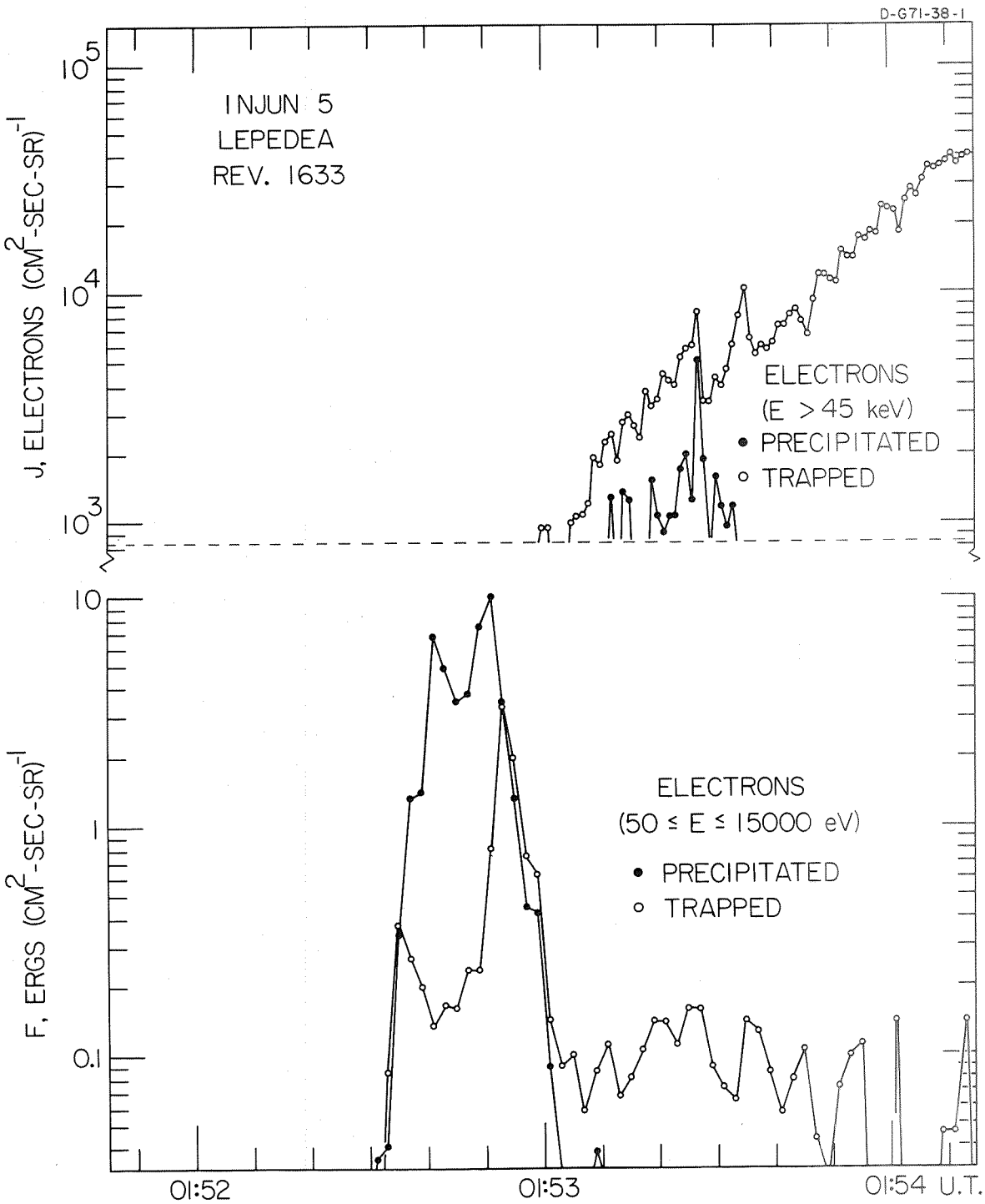
D-G71-38-1
INJUN 5
LEPEDEA
REV. 1633
J, ELECTRONS (CM^2-SEC-SR)$^{-1}$
10^5
10^4
10^3
ELECTRONS
(E > 45 keV)
• PRECIPITATED
○ TRAPPED
F, ERGS (CM^2-SEC-SR)$^{-1}$
10
1
0.1
ELECTRONS
(50 ≤ E ≤ 15000 eV)
• PRECIPITATED
○ TRAPPED
01:52
01:53
01:54 U.T.

Figure 3.